Control of SiC based front-end rectifier under unbalanced supply voltage

R. Maheshwari, I. Trintis, G. Gohil, S. K. Chaudhary and S. Munk-Nielsen

- ***Published in:*** 17th European Conference on Power Electronics and Applications (EPE'15 ECCE-Europe), Geneva, 2015
- ***DOI:*** doi: 10.1109/EPE.2015.7309446
- ***Publication date:*** 2015
- ***Citation for published version:*** R. Maheshwari, I. Trintis, G. Gohil, S. K. Chaudhary and S. Munk-Nielsen, "Control of SiC based front-end rectifier under unbalanced supply voltage," 2015 17th European Conference on Power Electronics and Applications (EPE'15 ECCE-Europe), Geneva, 2015, pp. 1-7.

Control of SiC Based Front-End Rectifier under Unbalanced Supply Voltage

Ramkrishan Maheshwari*, Ionut Trintis†, Ghanshyamsinh Gohil†,
Sanjay Kumar Chaudhary, Stig Munk-Nielsen†
*Dept. of Electrical Engineering
Indian Institute of Technology, Delhi
New Delhi, India
†Dept. of Energy Technology
Aalborg University
Aalborg, Denmark
Tel.: +91 11 2659 7951
E-Mail: rkmahesh@ee.iitd.ac.in
URL: http://ee.iitd.ac.in

Keywords

Front-end rectifier, SiC converter, Unbalanced supply voltage

Abstract

A voltage source converter is used as a front end converter typically. In this paper, a converter which is realized using SiC MOSFET is considered. Due to SiC MOSFET, a switching frequency more than 50 kHz can be achieved. This can help increasing the current control loop bandwidth, which is not possible with the Si based converter switching with 10 – 20 kHz. Due to increased current controller bandwidth, it is possible to control the negative sequence current without a separate negative sequence current controller. This paper presents a new feedforward controller for the negative-sequence current together with a positive-sequence current controller for the front-end rectifier. A gain in the feedforward term can be changed to control the negative-sequence current. Simulation results are presented to verify the theory.

Introduction

A front-end converter is required for sinusoidal input current at unity power factor and realized by a voltage source converter. Typically, the converter is realized using Si based semiconductor devices. However, novel power devices based on wide-bandgap (WBG) semiconductors have become commercially available recently. Using these devices, it is possible to increase the voltage blocking capability of the majority carrier devices which can switch faster [1], [2]. In addition, these devices can operate with higher junction temperature compared to Si devices [1], [2]. Due to this, the weight and volume of the power converter can be reduced.

The Si based converters switch with 10-30 kHz switching frequency. Therefore, the filter required at the input is typically LCL filter [3]. However, a SiC based converter can switch with 50-500 kHz. Such increase in the switching frequency enables the use of smaller choke inductor. So 1% inductive filter can provide sufficient filtering of the input current. This changes the system parameter and the crossover frequency of the plant transfer function which need to be controlled.

To achieve unity power factor, several control algorithms are proposed. Typically, a synchronous dq-reference frame based controller is used [4]. This controller requires a dc value of the reference and the feedback current. However, the feedback current may have a 100 Hz component due to a negative-sequence component of the grid power supply due to unbalance. Therefore, a low pass filter is required to get the dc value of the feedback current [5]. This low-pass filter causes slow dynamic performance of the current controller. In addition, a separate negative-sequence current controller is required to control negative-sequence component of the current. [5]-[6].

These control algorithms are designed for Si based converters. But in the case of a SiC converter switching at 50-500 kHz, controller with high bandwidth can be implemented. This paper utilizes this advantage and proposes the use a feedforward term to control the negative-sequence component of current without compromising the dynamic behavior. A feedforward term uses a high-pass filter and a gain to control the negative-sequence current. It does not require any low-pass filter in the feedback path. Therefore, a high bandwidth current controller can be implemented.

The system description is presented in Section II. For the presented system, a control with feedforward is proposed in Section III. The feedforward term consist of a high-pass filter followed by a gain. The gain can be changed to control the negative-sequence current. The simulation results for two different value of gain is presented in Section IV. A hardware is being developed using SiC MOSFET based module. The experimental results are presented in Section V. The conclusion is presented in Section VI.

System description and model

A block schematics of a front-end converter is shown in Fig. 1. A three-phase voltage source converter is connected to the grid using an inductive filter. In this paper, SiC based three-phase converter is considered. The resistance and the inductance of the inductor is represented by R_f and L_f, respectively. The dynamic equation of the inverter ac side currents in an arbitrary rotating *dq*-reference frame is given by

$$\begin{aligned} L_f \frac{d}{dt} i_{sd} + R_f i_{sd} &= v_{gd} - v_{invd} + \omega L_f i_{sq} \\ L_f \frac{d}{dt} i_{sq} + R_f i_{sq} &= v_{gq} - v_{invq} - \omega L_f i_{sd} \end{aligned} \tag{1}$$

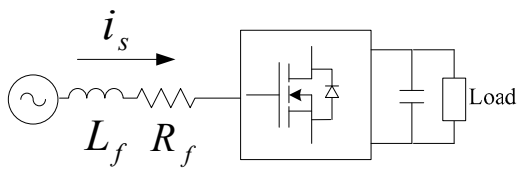

Fig. 1. Block schematics of front–end converter.

The *d*-axis is in-phase with the grid voltage space vector. This means that the active power supplied by the grid is equal to the product of *d*-axis component of the grid voltage and current. Therefore, the *d*-axis current reference should be controlled to control the power, and the *q*-axis current reference should be zero. The *d*-axis current reference is the output of the outer dc-link voltage control loop as shown in Fig. 2. A slow outer control loop dynamics is required since the grid current consist of the negative-sequence current. The negative-sequence current drawn from the grid will cause low frequency oscillation in the dc-link capacitor. Therefore, the dc-link capacitance value should be chosen in a way that the low frequency oscillations should remain within specification.

The front-end converter is realized by SiC based MOSFET. The power rating of the front-end converter is 5 kW for a low voltage grid (400 V_{L-L}). Since the switching frequency of the converter is 50 kHz, the inductance of the choke can be chosen as 1 pu which is equal to 1 mH in this case. The resistance of the series path (R_f) is chosen as 0.5 Ω. The 1 pu inductor is not possible in case of a Si based converter. This enables the use of feedforward term described in the following section.

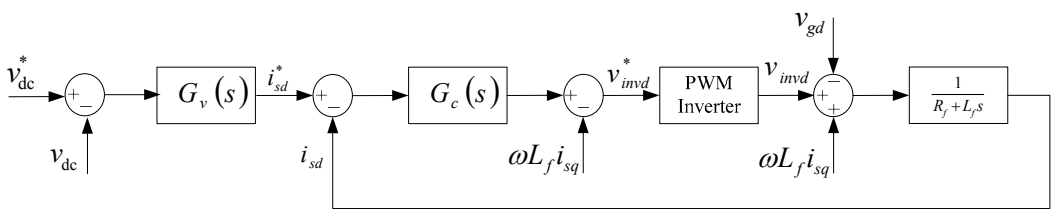

Fig. 2. Block diagram of the *d*-axis current controller.

Control with feedforward term

A typical control block diagram for the control of the d-axis current is shown in Fig. 2. The outer dc-link voltage controller provides the reference current for d-axis current. A simple proportional-integral controller $G_c(s)$ is used as the current controller as given by

$$G_c(s) = \frac{\omega_c (R_f + L_f s)}{s} \tag{2}$$

In Fig. 2, if the gain of the SiC based converter gain is assumed to be one, the current control loop block diagram reduces to a block diagram as shown in Fig. 3. Therefore, the input-to-output transfer function is given by

$$\frac{i_d(s)}{i_d^*(s)} = \frac{1}{1 + \frac{s}{\omega_c}} \tag{3}$$

where ω_c is the desired bandwidth of the control system. In this case, ω_c is chosen as 5 kHz since a SiC based converter with switching frequency equal to 50 kHz is used. This is the major difference as compared to standard grid-connected converter. The standard Si based converter has switching frequency in the range of 10-30 kHz. Therefore, it is not possible to have ω_c equal to 5 kHz.

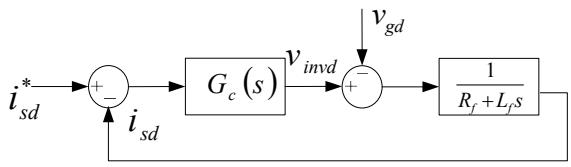

Fig. 3. Reduced block diagram of the current control

In Fig. 3, the *d*-axis component of grid voltage (v_{gd}) can be considered as a disturbance, and the effect of v_{gd} on the output i_{sd} is governed by the disturbance-to-output transfer function which is given by

$$\frac{i_{sd}(s)}{v_{gd}(s)} = -\frac{1}{G_c(s)} \frac{1}{1 + \frac{s}{\omega_c}} \tag{4}$$

For dc value of v_{gd} (ideal three-phase balanced grid voltage supply), the output i_{sd} due to v_{gd} will be zero since the dc gain of the PI controller infinite. However, in case of unbalance grid voltage supply, the output i_{sd} due to v_{gd} depends on the transfer function given by (4). The unbalanced grid voltage supply implies that there exist a negative sequence component, which is 100 Hz component of v_{gd}. It should be noted that only the negative sequence component is considered for demonstrating the

effectiveness of the proposed method. For the system parameter given in the previous section, the output i_{sd} due to the 100 Hz component of v_{gd} is given by

$$\frac{\underline{\boldsymbol{i}}_{\boldsymbol{d}}(j200\pi)}{\underline{\boldsymbol{v}}_{\boldsymbol{gd}}(j200\pi)} = -\frac{1}{\underline{\boldsymbol{G}}_{\boldsymbol{c}}(j200\pi)} = -\frac{1}{\omega_c L_f}\angle 0° \tag{5}$$

To control the negative sequence component, a voltage feedforward term can be added in the current control loop. The feedforward term consist of a high-pass filter followed be a gain k, as shown in Fig. 4. In Fig. 4, if the gain of the SiC based converter gain is assumed to be 1, the block diagram reduces to a block diagram as shown in Fig. 5. This do not change the dynamics of the input-to-output transfer function, but it changes the disturbance-to-output transfer function as given by

$$\frac{i_{sd}(s)}{v_{gd}(s)} = \frac{1}{G_c(s)}\frac{k-1}{1+\frac{s}{\omega_c}} \tag{6}$$

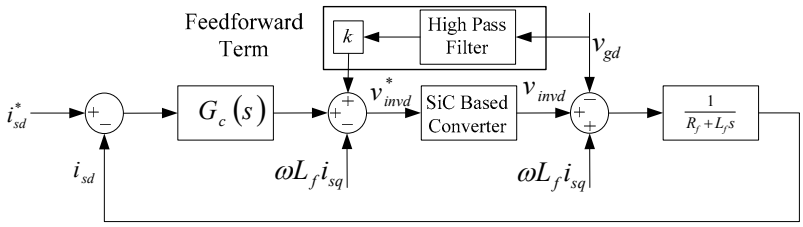

Fig. 4. Modified current control with feedforward

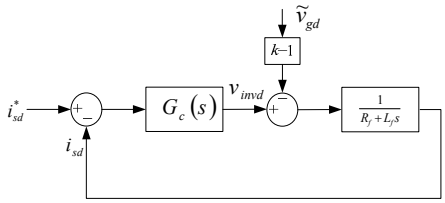

Fig. 5. Reduced current control block diagram with feedforward

Therefore, the output i_{sd} due to the 100 Hz component of v_{gd} is given by

$$\frac{\underline{\mathbf{i}}_{\mathbf{d}}(j200\pi)}{\underline{\mathbf{v}}_{\mathbf{gd}}(j200\pi)} = \frac{k-1}{\underline{\mathbf{G}}_{\mathbf{c}}(j200\pi)} = \frac{k-1}{\omega_c L_f}\angle 0° \tag{7}$$

and the 100 Hz component of the output i_{sd} depends on value of gain k. For $k = 1$, the output i_{sd} due to the 100 Hz component of v_{gd} will be zero and the front-end converter will draw balanced three-phase current even in the presence of the negative-sequence component in the grid voltage supply. By changing the value of k, the negative-sequence component of the three-phase grid current can be controlled. This feature can be used to support the grid in case of unbalance. During unbalance, a phase voltage amplitude will be less than other phase. It is desired to draw high current from the phase which has high amplitude. Depending on the required negative sequence current, a proper value of the gain k can be selected. As an example, if the positive and the negative-sequence component of the grid currents are required to be equal, the gain k can be given by

$$k = \frac{i_{sd}^* L_f \omega_c}{\sqrt{\left|\underline{\boldsymbol{v}}_{\boldsymbol{gd}}(j200\pi)\right|^2 + \left|\underline{\boldsymbol{v}}_{\boldsymbol{gq}}(j200\pi)\right|^2}} + 1 \tag{8}$$

Simulation Results

The abovementioned system is simulated in MATLAB SIMULINK® to prove the algorithm. 230 V three-phase grid voltage supply is used for the simulation. Reference currents for the *d*- and *q*- axis are 10 A and 0 A, respectively. The grid supply has 2% unbalance which can be seen as 100 Hz component in the *d*- and *q*- axis grid voltages. The value for the feedforward gain is selected as 1 (k = 1). The simulation results are shown in Fig. 6. The results show that the grid current is balanced even in the presence of unbalance grid supply voltage.

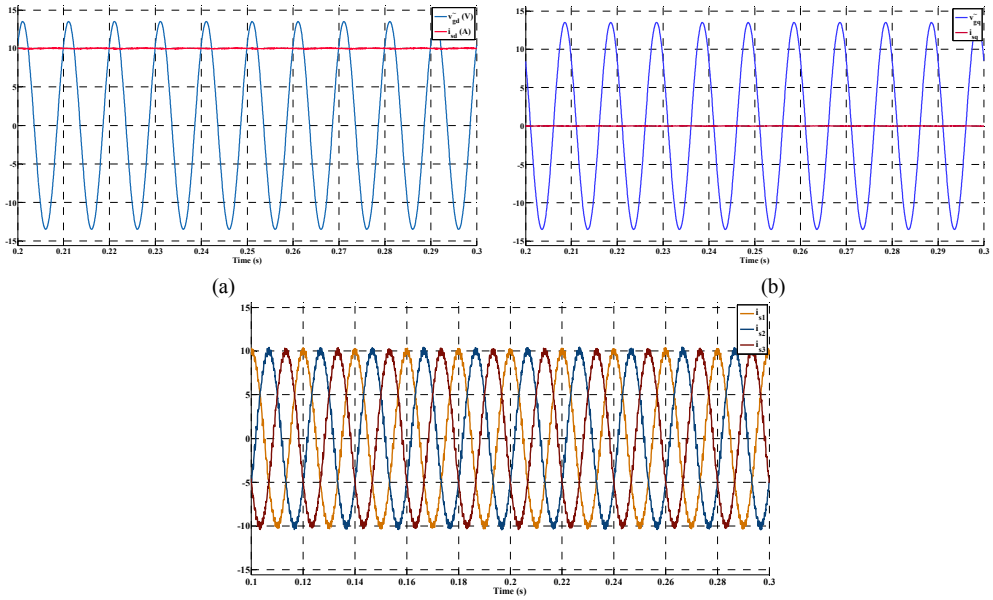

Fig. 6. (a) *d*-axis grid voltage ripple and grid current, (b) *q*-axis grid voltage ripple and grid current, and (c) grid current in stationary reference frame for 2% unbalance in the grid supply and k = 1

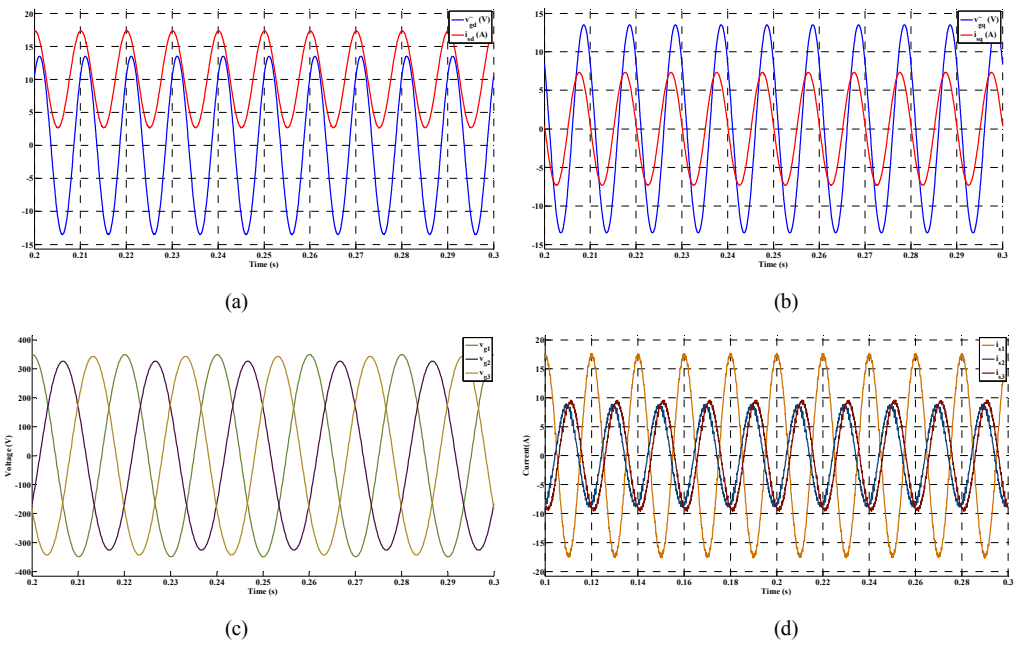

Fig. 7. (a) *d*-axis grid voltage ripple and grid current, (b) *q*-axis grid voltage ripple and grid current, (c) grid supply voltage, and (d) grid current in stationary reference frame for 2% unbalance in the grid supply and k is given by (8)

Under same grid conditions and the current reference settings, the value of k is changed to as given by (8). The simulation results are shown in Fig. 7. In this case, the magnitude of the negative-sequence current is equal to the positive-sequence current. The phase which has high voltage magnitude is loaded more in this case. This way the unbalance in the system can be reduced.

Experimental Results

A hardware setup with SiC based inverter is developed. The converter is connected to a three-phase programmable power supply through 1 mH inductor. The converter is controlled as a rectifier which is supplied by a grid voltage with 2% unbalance. Reference currents for the d- and q- axis are 10 A and 0 A, respectively. The experiments are conducted under the condition of 2% unbalance in the grid. The switching frequency of the converter is 50 kHz. The experimental results are shown in Fig. 8. The grid supply voltage is shown in Fig. 8(a). The grid currents are shown in Fig. 8(b) and (c) for $k = 1$ and 15. The phase which has maximum voltage amplitude draws the maximum current. This can help reducing the unbalance in the system.

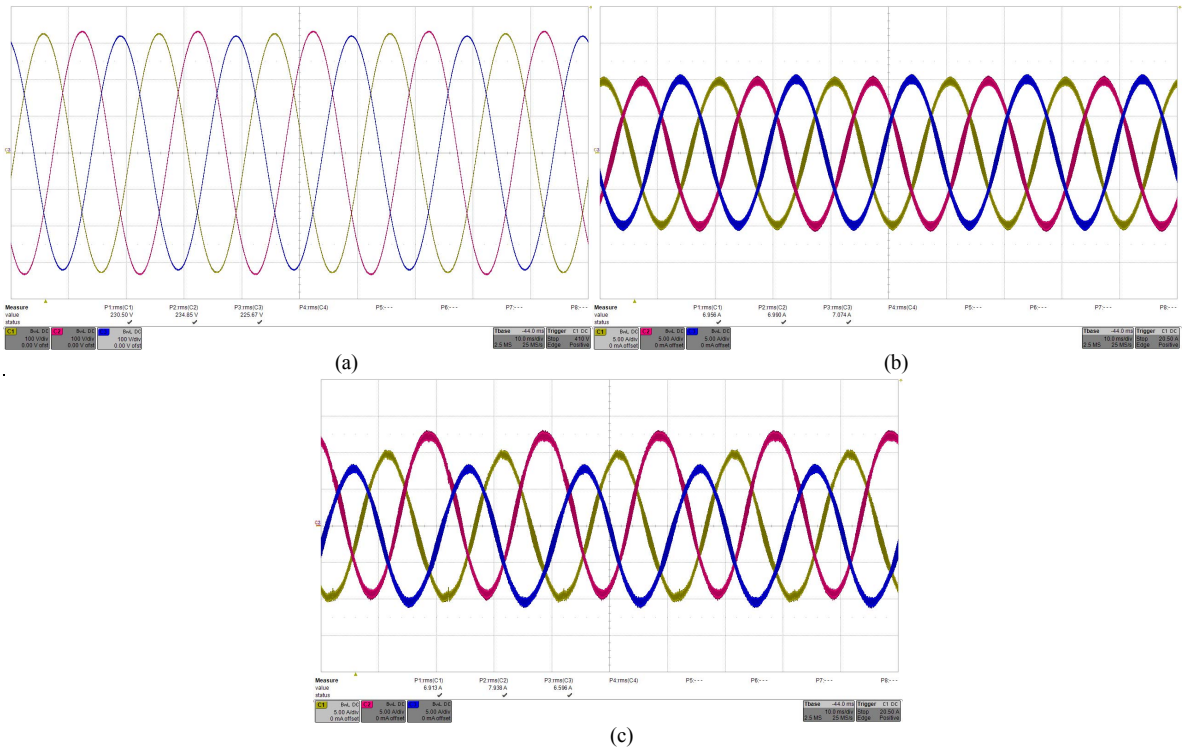

Fig. 8. (a) Grid supply voltage with 2% unbalance and grid currents for (b) $k = 1$ and (c) $k = 15$.

Conclusion

A SiC based front-end converter controller is proposed in this paper. A feedforward term is used in this paper to control the negative-sequence current from the grid. The feedforward term require one high pass filter and a gain. This implementation is very easy and can be incorporated in an existing controller. This control does not require any filter on the current feedback path. Therefore, the dynamic of the current control loop can be very fast. The current control loop has the bandwidth of 5 kHz since the converter switching frequency is 50 kHz. The feedforward term controls the negative sequence current in such a way that the phase with the maximum voltage value draws the maximum current. The simulation and experimental results validate the controller performance.

References

[1] Millan J., Godignon P., Perpina X., Perez-Tomas A., and Rebollo J.: A survey of wide bandgap power semiconductor devices, IEEE Trans. on Power Electron. vol. 29 no. 5 pp. 2155-2163 May 2014

[2] Hudgins J. L., Simin G. S., Santi E., and Asif Khan M.: An assessment of wide bandgap semiconductors for power devices, IEEE Trans. on Power Electron. vol. 18 no. 3 pp. 907-914 May 2003

[3] Liserre M., Blaabjerg F., and Hansen S.: Design and control of an LCL-filter-based three-phase active rectifier, IEEE Trans. on Ind. Appl. vol.41 no.5 pp. 1281-1291 Sept.-Oct. 2005

[4] Rowan T. M., and Kerkman R. J.: A new synchronous current regulator and an analysis of current-regulated PWM inverters, IEEE Trans. on Ind. Appl. vol.IA-22 no.4 pp.678-690 July 1986

[5] Guowei Z., Tongzhen W., Shengli H., and Lingzhi K.: The control for grid connected inverter of distributed generation under unbalanced grid voltage, SUPERGEN 09 pp.1-7 April 2009

[6] Song H. S. and Nam K.: Dual current control scheme for PWM converter under unbalanced input voltage conditions, IEEE Trans. on Ind. Electron. vol.46 no.5 pp.953-959 Oct 1999